Article

Not peer-reviewed version

Dirac Fermion of a Monopole Pair (MP) Model

Samuel Yuguru *

Posted Date: 18 June 2024

doi: 10.20944/preprints202210.0172.v10

Keywords: Dirac fermion; Dirac belt-trick; quantum mechanics; Dirac field theory

 doi:10.20944/preprints202210.0172.v10

Article

Dirac Fermion of a Monopole Pair (MP) Model

Samuel. P. Yuguru

Department of Chemistry, School of Natural and Physical Sciences, University of Papua New Guinea, P. O. Box 320, Waigani Campus, National Capital District 134, Papua New Guinea, samuel.yuguru@upng.ac.pg; Tel.: +675 326 7102; Fax: +675 326 0369

Abstract: The electron of spin −1/2 is a Dirac fermion of a complex four-component spinor field. Though it is effectively addressed by relativistic quantum field theory, an intuitive form of the fermion still remains lacking and it is often described by the so-called Dirac belt trick. In this novel undertaking, the electron is examined within the boundary posed by a recently proposed MP model of a hydrogen atom into 4D space-time that somewhat mimics Dirac string. Its transformation to Dirac fermion appears consistent with Dirac belt trick and quantum mechanics, whereas its solenoidal property for the emergence of monopole is applicable to Lie group. These outcomes are compatible with the basic interpretations of Dirac field theory and its related components like wave function collapse, quantized Hamiltonian, non-relativistic wave function, Weyl spinor, Lorentz transformation and electroweak symmetry breaking mechanism. The model though speculative, it could become important towards defining the fundamental state of matter subject to further examinations by conventional methods.

Keywords: dirac fermion; dirac belt-trick; quantum mechanics; dirac field theory

1. Introduction

At the fundamental level of matter, particles are described by wave-particle duality, charges and their spin property. These properties are revealed from light interactions and are pursued by the application of relativistic quantum field theory (QFT) [1,2]. The theory of special relativity defines lightspeed, c to be constant in a vacuum and its particle-like property consist of massless photon of spin 1 with a neutral charge. Any differences to photon's spin, charge and mass-energy equivalence by, $m = E/c^2$ provide the inherent properties of matter particles such as fermions of spin ±1/2 and this is termed causality [3,4]. Based on QFT, particles appear as excitation of fields permeating space at less than lightspeed. Within the atom, the electron is a fermion and its position is defined by non-relativistic Schrödinger's wave function, ψ of probabilistic distribution [5]. A level of indetermination is associated with the observation of its charge-spin property, whereas the wave-particle duality is depended on the instrumental set-up [6,7]. Based on quantum mechanics interpretation, the atom radiates energy in quantized form, nhv of infinitesimal steps. When this is incorporated into QFT, it becomes difficult to imagine wavy form of particles such as electrons freely permeating space without interactions and this somehow collapses to a point at observation [8]. Similarly, the resistive nature of proton decay [9] somehow suggests the preservation of the electron and hence, atom to balance out the charges. While proton decay is an active topic of research, in the meantime, the preferred quest is to make non-relativistic equations become relativistic due to the shared properties of both matter and light at the fundamental level as mentioned above.

Beginning with Klein-Gordon equation [10], the energy and momentum operators of Schrödinger equation,

$$\hat{E} = i\hbar\frac{\partial}{\partial t}, \qquad \hat{p} = -i\hbar\boldsymbol{\nabla}, \tag{1}$$

 doi:10.20944/preprints202210.0172.v10

are adapted in the expression,

$$\left(\hbar^2\frac{\partial^2}{\partial t^2} - c^2\hbar^2\boldsymbol{\nabla}^2 + m^2c^4\right)\psi(t,\bar{x}) = 0. \quad (2)$$

Equation (2) incorporates special relativity, $E^2 = p^2c^2 + m^2c^4$ for mass-energy equivalence, $\boldsymbol{\nabla}$ is the del operator in 3D space, $\hbar$ is reduced Planck constant and i is an imaginary number, $i = \sqrt{-1}$. Only one component is considered in Equation (2) and it does not take into account the negative energy contribution from antimatter. In contrast, the Hamiltonian operator, $\hat{H}$ of Dirac equation [11] for a free particle is,

$$\hat{H}\psi = (-i\boldsymbol{\nabla}.\boldsymbol{a} + m\beta)\psi. \quad (3)$$

The ψ has four-components of fields, i with vectors of momentum,∇ and gamma matrices, α, β represent Pauli matrices and unitarity. The concept is akin to, $e^+ e^- \longrightarrow 2\gamma$, where the electron annihilates with its antimatter to produce two gamma rays. Antimatter existence is readily observed in both Stern-Gerlach experiment and positron from cosmic rays. Suppose the electron is the quantized state of the electron field, the argument is made for the co-existence of monopole as the quantized state of the magnetic field and these are combined by Maxwell equation of electromagnetism. Monopole existence in experiments is confined to condensed matter and it cannot be extracted for measurements compared to the electron. The electron itself is a complex four-component spinor and it resumes its spin property at 720° rotation instead of 360° rotation. The process is described by the so-called Dirac belt trick [13] and is also referred to as the Balinese cup trick [14] or Dirac scissors problem [15] with other relatable descriptions include the Klein bottle topology [16]. At 360° rotation, maximum twist is attained and the unfolding process at another 360° rotation restores the electron or fermion to its original state. To complement the Dirac belt trick, a bar of magnet is envisioned to stretched out to form Dirac string and its excitation is expected to generate monopoles [15]. Because monopole existence is yet to be isolated from matter during observations, QFT such as Dirac theory is limited to describing fermions and bosons as unveiled by experiments.

In this novel study, how the electron orbits a monopole pair (MP) model of Dirac string is presented. Its transformation to Dirac fermion appears consistent with Dirac belt trick and quantum mechanics, while its solenoidal property into *n*-dimensions within the model is relevant to monopole emergence and Lie group application. These outcomes are compatible with the basic interpretations of Dirac field theory and its associated components like wave function collapse, quantized Hamiltonian, non-relativistic wave function, Weyl spinor, Lorentz transformation and electroweak symmetry breaking mechanism. Though the model remains a speculative tool, it is shown in this study that it could become important towards defining the fundamental state of matter subject to further examinations in both experiment and theoretical applications.

2. An Electron Conversion to a Fermion by Dirac Process

In this section, the transformation of a lone electron in a hydrogen atom type to a fermion by Dirac process is speculated within a spherical MP model of Dirac string (Figs. 1a–d). The process includes examination of Dirac belt trick by assuming the conservation of the atom, where the electron or its particle-hole by ionization balances out the proton charge. How these apply to quantum mechanics and the basics of QFT are demonstrated ensued by the solenoidal property into *n*-dimensions of the model and how this is relevant to the Lie Group. A summary is offered at the end before examining the model's compatibility to various aspects of Dirac field theory and its related components.

Unveiling Dirac Belt Trick within the Spherical MP Model

The electron's orbit of time reversal in discrete continuum form of sinusoidal wave is defined by Planck radiation, *h*. In forward time, the orbit is transformed into an elliptical shape of a MP pair field somewhat mimicking Dirac string (Figure 1a). It is dissected perpendicular by Bohr orbits (BOs) into *n*-dimensions of energy levels. By clockwise precession, the torque or right-handedness exerted on

Preprints.org (www.preprints.org) | NOT PEER-REVIEWED | Posted: 18 June 2024 doi:10.20944/preprints202210.0172.v10

the MP field shifts the electron of spin up from positions 0 to 4 to assume 360° rotation. Time reversal orbit against clockwise precession allows for maximum twist at the point-boundary or vertex of the MP field at position 4. The electron then flips to spin down mimicking a positron to begin the unfolding process and emits radiation by, $E = nhv$. The positron is short-lived from possible repulsion of the proton and by another 360° rotation from positions 5 to 8, the electron is restored to its original state. These intuitions are relatable to Dirac

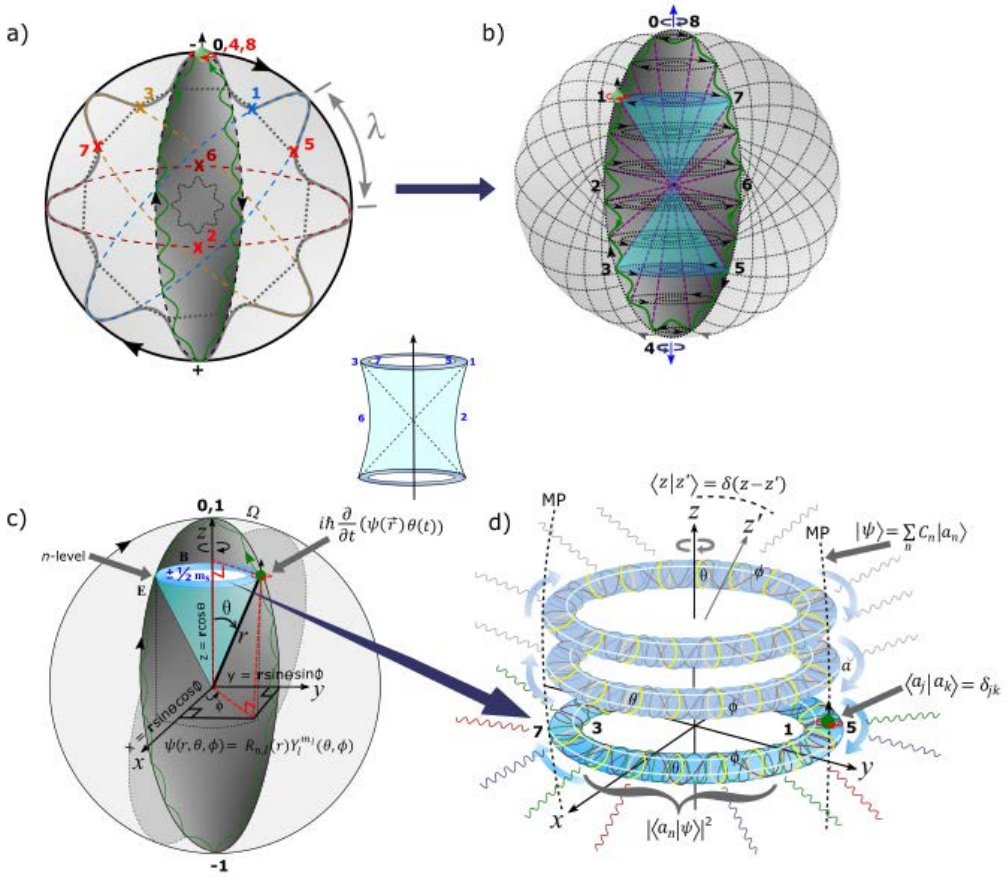

Figure 1. The MP model [17]. (a) In flat space, a spinning electron (green dot) in orbit of sinusoidal form (green curve) is of time reversal. It is normalized to an elliptical MP field (black area) of a magnetic field, **B** mimicking Dirac string. By clockwise precession (black arrows), an electric field, **E** of inertia frame, λ is generated. The shift in the electron's position from positions 0 to 4 at 360° rotation against clockwise precession offers maximum twist. At position 4, the electron flips to a positron to begin the unfolding process from positions 5 to 8 for another 360° rotation to restore the electron to its original state analogous to Dirac belt trick. For the total of 720° rotation, a dipole moment (±) is generated for the classical spherical model. (b) The BOs defined by conjugate numbered pairs, 1,3 and 5,7 translate to angular momentum (purple dotted lines) of spin ±1/2 depicted by a pair of light cones (navy colored) in Minkowski space-time. These are projected in degeneracy toward singularity at the center. (c) Lie Group. The electron in its orbit is tangential to smooth manifolds of both BOs and the spherical model. By precession, Ω, the model is polarized to generate qubits, 0 and ±1 at spherical lightspeed. The polar coordinates (r, θ, Φ) are attributed to Schrödinger wave function with respect to the electron's position in space. (d) Topological torus emerges from BOs defined by ϕ (white loops) and their dissection perpendicularly by θ (yellow circles) from intermittent clockwise precession stages of the MP field. Any light-matter interactions are tangential to the electron's position as the base point of the manifolds and these are transformed by linearization along the principle axis or *z*-axis of the MP field. Singularity at the center for the light-cone is out of reach due to the electron's shift at positions, 2 and 6 along horizontal *x*-*y* plane of an irreducible spinor field (insert centered image). The embedded terms and equations are explained in the text.

 doi:10.20944/preprints202210.0172.v10

Belt trick at 720° rotation, where the Dirac four-component spinor, $\psi = \begin{pmatrix} \psi_0 \\ \psi_1 \\ \psi_2 \\ \psi_3 \end{pmatrix}$ is assigned to positions 0 to 3 and its transposition to positions 4 to 8 at spherical lightspeed. In Minkowski space-time, the conjugate pairs of positions, 1, 3 and 5,7 offer light-cone depicting Weyl spinor of 4D space-time (Figs. 1b). The point of singularity for the light-cone is out of reach due to the electron's shift at positions, 2 and 6 for the irreducible spinor field (centered image of Figs. 1a–d). Additional details on the conceptualization path of the model from electron wave-diffraction is offered elsewhere [17]. Clockwise precession at spherical lightspeed presents an inertia reference frame, λ (Figure 1a) under the conditions,

$$\lambda_{\pm}^2 = \lambda_{\pm} \quad Tr\lambda_{\pm} = 2\,\lambda_{+} + \lambda_{-} = 1, \tag{4}$$

where the trace function, *Tr* is the sum of all elements within the model. These elements are applicable to both quantum mechanics and QFT including the Lie group as presented next.

Quantum Mechanics and Dirac Notations

The transformation of the electron to a Dirac fermion within the MP model can further accommodate some basic concepts in quantum mechanics and QFT (Figs. 1c and 1d). Some of them are outlined below in bullet points based on ref. [18].

- The electron of wave-particle duality obeys de Broglie relationship, $\lambda = \hbar/mv$ with h assigned to its sinusoidal orbit and mv to BO. It is defined by the wave function, ψ and its orbit of time reversal adheres to the Schrödinger equation, $i\hbar\frac{\partial}{\partial t}(\psi(\vec{r})\theta(t))$ in space-time (Figure 1c) (see also Appendix A for further explanations). Its superposition state (electron-positron pair) in space is linked to BO defined by ϕ and thus, its inner product is, $\langle\psi|\phi\rangle^* = \langle\psi|\phi\rangle$ with respect to z-axis. Conjugate charges at positions, 1, 3 and 5 and 7 cancels each other out at spherical lightspeed to form close loops, where the electron is stabilized to generate only either spin up or spin down in its orbit at an energy n-level in accordance with Pauli exclusion principle. At 360° rotation, an electron of spin up is produced and at 720° rotation, a positron of spin down is formed. The loops of BOs are topology construct of differential manifolds into n-levels or n-dimensions (Figure 1d). In this way, the electron forms a weak isospin, whereas the z-axis mimicking spin up and spin down resembles nuclear isospin.
- Both radial and angular wave functions are applicable to the electron, $\psi(r,\theta,\phi) = R_{n,l}(r)Y_l^{m_l}(\theta,\phi)$. The radial part, $R_{n,l}$ is attributed to the principal quantum number, n and angular momentum, l of a light-cone with respect to r (Figure 1c). The angular part, $Y_l^{m_l}$ in degenerate states, $\pm m_l$ with respect to the z-axis is assigned to the BO defined by both θ and ϕ (Figure 1d).
- The BO is defined by a constant structure, a and its orthogonal (perpendicular) to z-axis by linearization (Figure 1d). Its link to electron-positron pair is, $\langle a_j|a_k\rangle = \int dx\psi_{a_j}^*(x)\psi_{a_k}(x) = \delta_{jk}$ for continuous derivation by rotation and is relevant to Fourier transform (see also Appendix B). Linear translation for the n-levels along z-axis can relate to the sum of expansion coefficients, C_n, where the electron's position offers an expectant value, $|\psi\rangle = \sum_n C_n/a_n\rangle$. Its probability is of the type, $\langle a_n|\psi\rangle^2$.
- The shift in the electron's position of hermitian conjugates by Dirac process, $P(0\rightarrow 8) = \int_\tau \psi^*\hat{H}\psi d\tau$ assumes Hamiltonian space with τ by precession (Appendix B). The complete spherical rotation towards the point-boundary for the polarization states, 0, 1 assumes U(1) symmetry and incorporates Euler's formula, $e^{i\pi} + 1 = 0$ in real space.
- Singularity at Planck's length is assigned to the point-boundary at position 0 and this promotes radiation of the type, $E = nhv$ by the electron-positron transition. Somehow it sustains the principle axis of the MP field as z-axis or nuclear isospin in asymmetry and this sustains $\pm h$ at spherical lightspeed.

 doi:10.20944/preprints202210.0172.v10

Lie Group

The geometry of the MP model is relevant to Lie group of differential smooth manifolds and this is attributed to both BO of a circle and the spherical model (Figure 1c). The BO in degeneracy is topological into n-dimensions and its transection by the electron in orbit from positions $0 \rightarrow 8$ appears tangential to the boundaries of the manifolds of non-abelian and this generates a solenoid with $\nabla . B = \mu_0 \rho$ (Figure 1d). The solenoid is reduced to singularity at position 0 and the electron is transformed to a monopole with $\nabla . B = 0$. Rotation matrices of the type, $Rr_{yz}(\theta)$ and $R_{zx}(\theta)$ is attributed to the MP field by precession with any shift in z-axis of nuclear isospin trivial, $\langle z|z'\rangle = \delta(z - z')$ (Figure 1d). The rotation matrix, $R_{xy}(\theta)$ is assigned to the BO into n-dimensions. These are relevant to describe both integer and half-integer spins such as, 0, 1/2 and 1 towards complete rotation at position 0 at the point-boundary. These attributes are presented in Figure 2A of Appendix B with some examples are explored in here based on refs. [19,20].

The electron of chirality is described by,

$$g \in G, \tag{5}$$

where g is the electron's position as subset of the space tangential to the manifolds and G represents the Lie group. For the conjugate numbered pairs, 1, 3 and 5, 7 of BO (Figure 1d), Equation (5) validates the operations,

$$g_{1,5} + g_{3,7} \in G \tag{6a}$$

and

$$g + (-g) = i, \tag{6b}$$

where i is spin matrix for both spin ±1/2 (Figure 2A). The form, $g_1 + g_3 \neq g_5 + g_7$ due to electron-positron ($\pm g$) transition and radiation loss, $E = nhv$ tangential to the manifolds. For linear transformation along z-axis in 1D space, the BOs are isomorphic with respect to the particle position, $|\psi\rangle = \sum_n C_n/a_n\rangle$ (Figs. 1d and 2A). By intermittent precession, the inner product of r is a scalar and relates to the boundary of the MP field in the form,

$$\vec{r}_1 \,.\, \vec{r}_2 = |\vec{r}_1 \,||\, \vec{r}_2| cos\theta \tag{7}$$

where rotation of both vectors preserve the lengths and relative angles (e.g., Figure 1c). By assigning rotation matrix, R to Equation (7), its transposition is,

$$(Rr_1)^T (Rr_2) = r_1^T r_2 I, \tag{8}$$

where the identity matrix, $I = R^T \times R$ by reduction (Figure 2A). The orthogonal relationship of BO to clockwise precession along z-axis at 90° for all rotations suggests, $R \in$ SO(3). The SO(3) group rotation for integer spin 1 in 3D space is,

$$R_{yz}(\theta) = \begin{pmatrix} 1 & 0 & 0 \\ 0 & cos\theta & -sin\theta \\ 0 & sin\theta & cos\theta \end{pmatrix} \begin{pmatrix} x \\ y \\ z \end{pmatrix}. \tag{9}$$

Equation (9) can also be pursued for integer spin 0 and higher spin particles. When rotating as 2 x 2 Pauli vector for SU(2) symmetry with respect to a light-cone of half-integer spin (Figure 1d), Equation (9) translates to the form,

$$\pm \begin{pmatrix} cos\frac{\theta}{2} & isin\frac{\theta}{2} \\ isin\frac{\theta}{2} & cos\frac{\theta}{2} \end{pmatrix} = \begin{pmatrix} z & x - y_i \\ x + y_i & -z \end{pmatrix} = \begin{vmatrix} \xi_1 \\ \xi_2 \end{vmatrix} |-\xi_2 \quad \xi_1|, \tag{10}$$

where ξ_1 and ξ_2 are Pauli spinors of rank 1 to rank 1/2 tensor relevant for Dirac matrices (Figure 2A). By orthogonal geometry, the column is attributed θ at n-levels along z-axis and the row to BO defined by ϕ in degeneracy. For ladder operators at n-dimension along z-axis, SU(2) is irreducible for the shift in θ and ϕ such as, $\binom{SU(2)}{n \times n} \neq \binom{SU(2)}{l \times l} \oplus \binom{SU(2)}{m \times m}$. Translation of SU(2) by accentuating

 doi:10.20944/preprints202210.0172.v10

precession at high energy like, $\binom{SU(2)}{2\times 2}\oplus\binom{SU(2)}{2\times 2}$ matrices is reduced to the upright MP field position (e.g., Figure 1b). For the particle's position, when $y = 0$, $z = x$ is a real number. At $x = 0$, $z = y$ becomes an imaginary number. The BO linked to the electron's position can be assigned to SO(2) group in 2D such as,

$$\begin{pmatrix} cos\theta & sin\theta \\ -sin\theta & cos\theta \end{pmatrix} \cong \begin{pmatrix} 1 & \theta \\ -\theta & 1 \end{pmatrix} = I + \theta \begin{pmatrix} 0 & 1 \\ -1 & 0 \end{pmatrix}, \tag{11}$$

where, $\theta \in [0,2\pi]$ incorporates Dirac process at 720° rotation (e.g., Figure 1a). Similar relationships can be forged for $R_{xy}(\phi)$ with respect to the BO along x-y plane with respect to Equation (9) in the form,

$$R_{xy}(\phi) = \begin{pmatrix} cos\phi & -sin\phi & 0 \\ sin\phi & cos\phi & 0 \\ 0 & 0 & 1 \end{pmatrix} \begin{pmatrix} x \\ y \\ z \end{pmatrix} = \pm \begin{pmatrix} e^{i\frac{\phi}{2}} & 0 \\ 0 & e^{-i\frac{\phi}{2}} \end{pmatrix}. \tag{12}$$

Substitution of Equation (12) with $R_{xy}(\phi) = e^{\theta}$ can relate to polarization states, -1, 1 and 0 at the vertices of the MP field (Figure 1c) from the electron-positron transition such as,

$$e^{\theta} \begin{bmatrix} 0 & -1 & 0 \\ 1 & 0 & 0 \\ 0 & 0 & 0 \end{bmatrix} = \begin{bmatrix} cos\theta & -sin\theta & 0 \\ sin\theta & cos\theta & 0 \\ 0 & 0 & 1 \end{bmatrix}. \tag{13}$$

The physical perspective of Equation (13) is provided in Figure 2A for the rotation of BOs into n-dimensions with respect to the emergence of solenoidal property. These explanations offer the basics to the complexities of compact Lie group similar to those demonstrated for quantum mechanics and Dirac notations in the preceding subsection.

Summary

The physicality of the electron within the MP model can assume both fermion and monopole characteristics. The former by Dirac process as described above (e.g., Figs. 1a and 1b) and the electron is expected to dominate to balance out the positive charge of the proton with positron emergence being transient. Polarization of the model by the electron transition in orbit can be described by both quantum mechanics and QFT and this generates electric dipole moment relevant to quantization of electric charge with $\nabla . E = \rho/\varepsilon_0$. When the electron is tangential to the vertex of the MP field at position 0, the acquired solenoidal property applicable to the Lie group into n-dimensions of BOs (Figure 1d) is reduced to a monopole and this is not transferrable by linearization. These descriptions are relevant to describing both the Higgs field and Coulomb's interaction. For example, the electron at position 0 intercepts the principle axis of the elliptical MP field into n-dimensions of BOs and this can accommodate a plethora of particle types from coupling of ionized models akin to proton-proton collisions. If center of mass (COM) is at position 0, by self-interaction it would mimic the Higgs field, $V(\phi) = m_H^2\phi^2 + \lambda\phi^4$ of a scalar quantity. The position is unidirectional by external interaction and this can further accommodate doublet to antidoublet fields. The first term, m_H^2 defines Higgs boson ($H°$) and it mimics the electron or its particle-hole symmetry by ionization of the model. The second term, $\lambda\phi^4$ incorporates the particle-hole shift at positions 1 and 3 by precession (Figure 1a). When zooming in towards position 0, the particle property is constrained but the potential well becomes infinite at positions 1 and 3 with momentum undefined in accordance with the uncertainty principle.

The COM at the vertex of the MP model is also relevant to Coulomb's law of electric force in a vacuum between two charged bodies, $F = \frac{1}{4\pi\varepsilon_0}.\frac{q_1.q_2}{r^2}$. The bodies could reflect the electron-positron transition by Dirac process towards position 0 at a distance, r assumed along the z-axis of the MP field (Figure 1a). The inertia frame can substitute for centripetal force by precession at a constant velocity. Such a notion considers gravity to be a classical force for an irreducible spinor field.

Preprints.org (www.preprints.org) | NOT PEER-REVIEWED | Posted: 18 June 2024 doi:10.20944/preprints202210.0172.v10

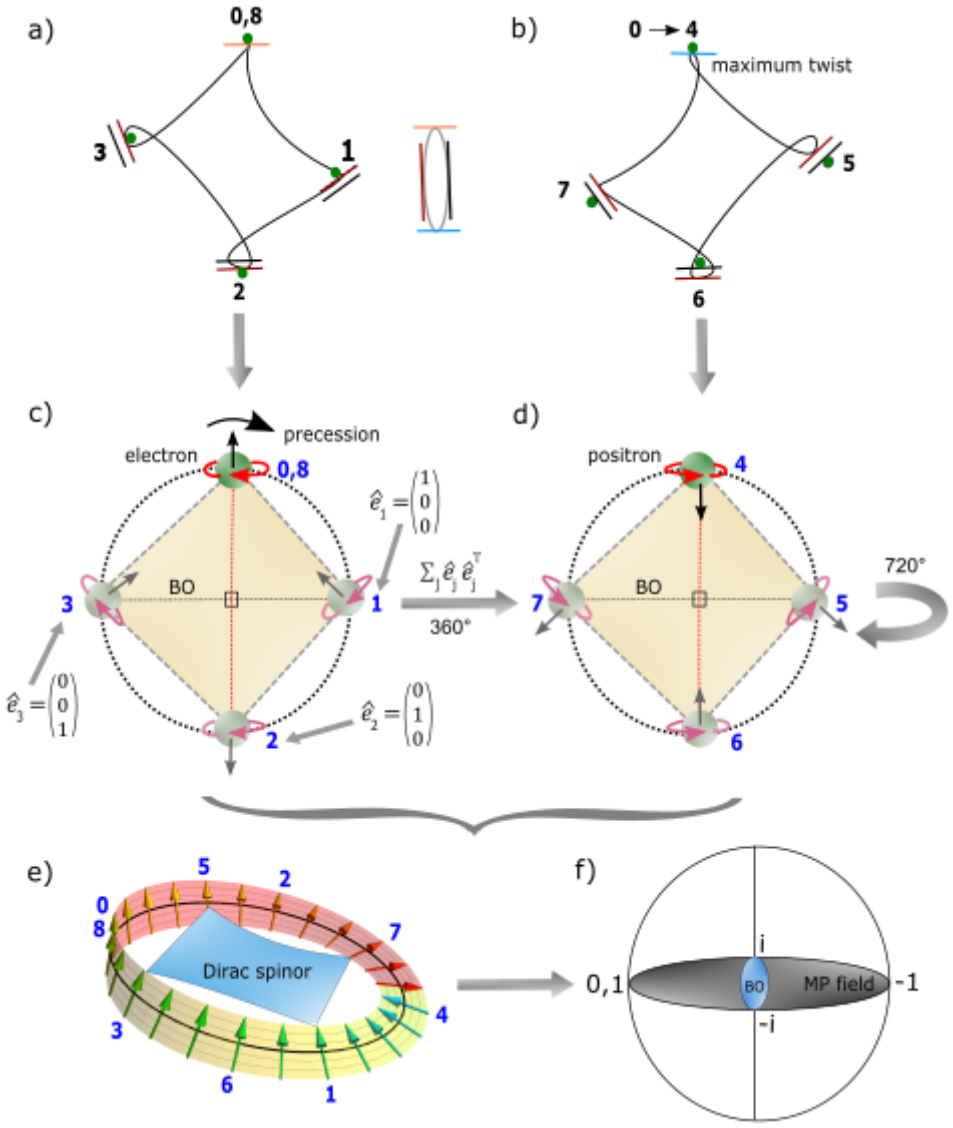

Figure 2. Dirac belt trick. (a) The electron's (green dot) induced rotation due to clockwise precession against its time reversal elliptical orbit insinuates a close loop within a *hemisphere* at spherical lightspeed based on the MP model (Figure 1a). The position of the particle on a straight path (colored lines) is referenced to the MP field of elliptical shape (centered image). (b) Maximum twist is attained at position 4 as detectable energy and the unfolding process offers another loop at 360° rotation for a total of 720° rotation to restore the electron at position 8 or 0 akin to Dirac belt trick. (c) Precession normalizes the loop to generate an electron of positive helicity or right-handedness. The spin up vector correlates with the direction of precession. (d) The electron flips to a positron of negative helicity or left-handedness. The spin down vector is in opposite direction to the direction of precession to begin the unfolding process. By transposition at 360° rotation, $\sum_j \hat{e}_j \hat{e}_j^T = [e_i e_j] = c_{ij}^k e_k$ with c_{ij}^k is expansion coefficients or structural constants, $\hat{e}_k$ is unit matrices and ij is the shift in the electron-positron transition. (e) Irreducible spinor field somewhat mimicking the MP field (e.g., Figure 1b). Cancelation of charges at conjugate positions, 1, 3 and 5, 7 at spherical lightspeed offers close loops of BOs to stabilize the electron to only generate either spin up or spin down states (e.g., Figure 1d). The point of singularity is evaded due to shift in the electron's position at 2 and 6, where the z-axis mimics nuclear isospin. The tilt at position 4 compared to position 0 is attributed to energy loss from the electron-positron transition in the form, $E = h\nu = g\beta B$. (f) Polarization of the model either horizontal or vertical with respect to the electron-positron pair, ±i generates qubits 0, ±1 at positions, 0, 4 and 8 (see also Figure 1a). Image (e) adapted from ref. [21].

 doi:10.20944/preprints202210.0172.v10

3. Dirac Field Theory and Its Related Components

Further exploration of the Dirac belt-trick into depth with respect to the MP model is offered in Figs. 2a–f. The electron's time reversal orbit of a MP field mimics Dirac string and it is subjected to both twisting and unfolding process by clockwise precession. Cancellation of charges at conjugate positions 1, 3 and 5, 7 allows for the emergence of BOs in manifolds and these generate either spin up or spin down states. How these are compatible with the basics of Dirac theory and its associated components [1,2,10,11] are succinctly described in bullet points for further undertakings.

Dirac theory and helical property. The fermion field is defined by the famous Dirac equation of the generic form,

$$i\hbar\gamma^u\partial_u\psi(x) - mc\psi(x) = 0, \tag{14}$$

where γ^u are gamma matrices. The exponentials of the matrices, $\{\gamma^o\gamma^1\gamma^2\gamma^3\}$ are attributed to the electron's position by clockwise precession acting on its time reversal orbit. For example, γ^o is assigned to the vertex of the MP field and by electron-positron transition at position 0, it sustains *z*-axis as arrow of time in asymmetry. The $\gamma^1\gamma^2\gamma^3$ variables of Dirac matrices are related to the electron shift in its positions (Figs. 2a–f). Orthogonal projections of the space-time variables, $\frac{1}{2}(1 \pm i\gamma^0\gamma^1\gamma^2\gamma^3)$ are confined to a hemisphere and assigned to a light cone (e.g., Figure 1c). These are incorporated into the famous Dirac equation,

$$\left(i\gamma^0\frac{\partial}{\partial t} + cA\frac{\partial}{\partial x} + cB\frac{\partial}{\partial y} + cC\frac{\partial}{\partial z} - \frac{mc^2}{\hbar}\right)\psi(t,\vec{x}), \tag{15}$$

where *c* acts on the coefficients A, B and C and transforms them to γ^1, γ^2 and γ^3. The exponentials of γ are denoted *i* for off-diagonal Pauli matrices for the light-cone (Figure 1d) and is defined by,

$$\gamma^i = \begin{pmatrix} 0 & \sigma^i \\ -\sigma^i & 0 \end{pmatrix}, \tag{16a}$$

and zero exponential, γ^o is,

$$\gamma^0 = \begin{pmatrix} 0 & 1 \\ 1 & 0 \end{pmatrix}. \tag{16b}$$

σ^i is relevant to oscillations assumed at the BOs (Figure 1d) with anticommutation relationship, $e^+(\psi) \neq e^-(\bar{\psi})$ of chiral symmetry (Figs. 2c and 2d). The associated vector gauge invariance for the electron-positron transition exhibits the following relationships,

$$\psi_L \rightarrow e^{i\theta L}\psi_L \tag{17a}$$

and

$$\psi_R \rightarrow e^{i\theta L}\psi_R. \tag{17b}$$

The exponential factor, $i\theta$ refers to the position, *i* of the electron of a complex number and θ, is its angular momentum (e.g., Figure 1c). The unitary rotations of right-handedness (*R*) or positive helicity and left-handedness (*L*) or negative helicity are applicable to the electron transformation to Dirac fermion (e.g., Figure 2A in Appendix B). The process is confined to a hemisphere and this equates to spin 1/2 property of a complex spinor. Two successive rotations of the electron in orbit by clockwise precession of the MP field is identified by $i\hbar$. The chirality or vector axial current at the point-boundary is assigned to polarized states, ±1 of the model (Figure 1c). The helical symmetry from projections operators or nuclear isospin of *z*-axis acting on the spinors (Figure 2e) is,

$$P_L = \frac{1}{2}(1 - \gamma_5) \tag{18a}$$

and

$$P_R = \frac{1}{2}(1 - \gamma_5), \tag{18b}$$

Preprints.org (www.preprints.org) | NOT PEER-REVIEWED | Posted: 18 June 2024 doi:10.20944/preprints202210.0172.v10

where γ_5 is likened to thermal radiation of a black body. The usual properties of projection operators are: $L + R = 1$; $RL = LR = 0$; $L^2 = L$ and $R^2 = R$ (e.g., Figs. 2a–d).

Wave function collapse. Dirac fermion or spinor is denoted $\psi(\mathbf{x})$ in 3D Euclidean space and it is superimposed onto the MP model of 4D space-time, $\psi(\mathbf{x},t)$ by clockwise precession (Figure 3a). The former of 3D includes both positive and negative curvatures of

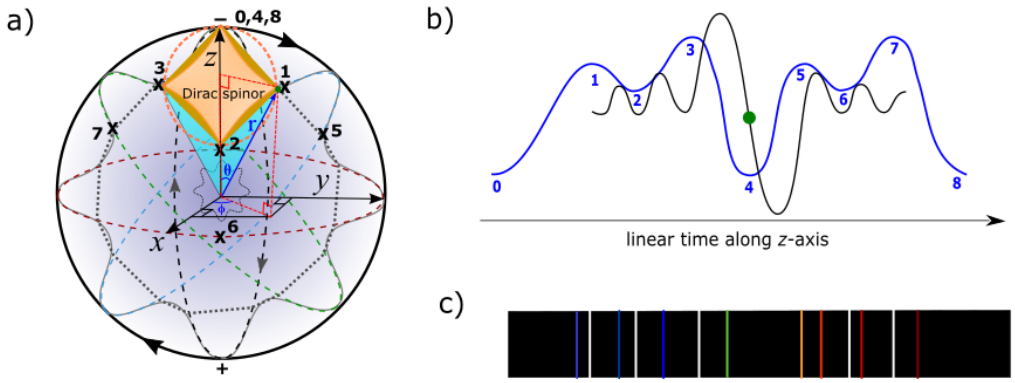

Figure 3. Wave function collapse. (a) Irreducible Dirac spinor is defined by vector space superimposed on Poincaré sphere. It consists of both Euclidean (straight paths) and non-Euclidean (negative and positive curves) spaces. Clockwise precession by geodesic motion induces a circle at 360° rotation to the negative curves at positions 0 to 3 (e.g., Figure 2c). The polar coordinates (r, θ, Φ) are linked to a light cone (navy colored). Position 6 is projected inwards from position 2. (b) By Fourier transform (blue wavy curve) into linear time, positions 2 and 6 constraints the reach of singularity. Zooming in towards the particle's position presents the Heisenberg uncertainty principle (black wavy curve) for the electron of superposition states linked to BO (e.g., Figure 1d). These can translate to (c) a typical hydrogen emission spectrum. The amplitudes by Fourier transform are shown by white spectral lines and the uncertainty principle with respect to the particle property by colored spectral lines (see also Appendices B and C). .

non-Euclidean space (e.g., Figs. 2a and 2b) normalized to straight paths of Euclidean space (Figs. 2c and 2d) and are imposed on the surface of Poincaré sphere defined by non-abelian Lie group (see subsection 2c). The latter of 4D resembles Minkowski space-time and consists of a light-cone dissected by z-axis as arrow of time. The Dirac four-component spinor, $\psi = \begin{pmatrix} \psi_0 \\ \psi_1 \\ \psi_2 \\ \psi_3 \end{pmatrix}$ is attributed to positions 0 to 3 of conjugate pairs in 3D space. Convergence of positions 1 and 3 at either position 0 or 2 is relevant to the equivalence principle based on general relativity. Any light paths tangential to the point-boundary of the n-energy manifolds of BOs is expected to transform the spinor into linear time mimicking Fourier transform for wave function collapse scenario (Figure 3b). Constraining the electron's position along the z-axis offers the uncertainty principle due to the particle's link to the BO. The wave amplitudes can relate to a typical hydrogen emission spectrum for external light-matter interactions with respect to the electron's position in orbit (Figure 3c). In this way, wave function collapse of probabilistic distribution by Born's rule, $|\psi|^2$, where the spherical model is reduced to linearization along z-axis.

Quantized Hamiltonian. Two ansatzes adapted from Equation (14) are given by,

$$\psi = u(\mathbf{p})e^{-ip.x}, \tag{19a}$$

and

$$\psi = v(\mathbf{p})e^{ip.x}, \tag{19b}$$

where outward project of spin at positions 5, 7 is represented by v and inward projection at positions 1, 3 by u (e.g., Figs. 2c and 2d). By linear transformation, the hermitian plane wave solutions form

 doi:10.20944/preprints202210.0172.v10

the basis for Fourier components in 3D space (Figs. 1d and 3b). Decomposition of quantized Hamiltonian [22] ensues as,

$$\psi(x) = \frac{1}{(2\pi)^{3/2}} \int \frac{d^3}{2E_{\mathbf{p}}} \sum_s \left(a_{\mathbf{P}}^s u^s(p) e^{-ip.x} + b_{\mathbf{P}}^{s\dagger} v^s(p) e^{ip.x} \right), \tag{20a}$$

where the constant, $\frac{1}{(2\pi)^{3/2}}$ is attributed to the dissection of BOs along z-axis. Its conjugate form is by,

$$\bar{\psi}(x) = \frac{1}{(2\pi)^{3/2}} \int \frac{d^3}{2E_{\mathbf{p}}} \sum_s \left(a_{\mathbf{P}}^{s\dagger} \bar{u}^s(p) e^{ip.x} + b_{\mathbf{P}}^s \bar{v}^s(p) e^{-ip.x} \right). \tag{20b}$$

The coefficients $a_{\mathbf{P}}^s$ and $a_{\mathbf{P}}^{s\dagger}$ are ladder operators for u-type spinor and $b_{\mathbf{P}}^s$ and $b_{\mathbf{P}}^{s\dagger}$ for v-type spinor at n-dimensions along BOs (e.g., Figure 1d). These related to Dirac spinors of two spin states, ±1/2 and $\bar{v}^s$ and $\bar{u}^s$ as their antiparticles. Dirac Hamiltonian of one-particle quantum mechanics relevant to the MP model of hydrogen atom type is,

$$H = \int d^3x \psi^\dagger(x) [-i\gamma^0 \gamma . \boldsymbol{\nabla} + m\gamma^0] \psi(x). \tag{21}$$

The quantity in the bracket is provided in Equation (3). By parity transformation, the observable and holographic oscillators are canonically conjugates (e.g., Figs. 2c and 2d). The associated momentum is,

$$\pi = \frac{\partial \mathcal{L}}{\partial \psi} - \bar{\psi} i\gamma^0 = i\psi^\dagger. \tag{22}$$

With z-axis of the MP field aligned to the vertex in asymmetry (Figure 1c), the V-A currents comparable to Fourier transform are projected in either x or y directions in 3D space (Figs. 1d and 3b). These assume the relationships,

$$\left[\psi_\alpha(\mathbf{x}, t), \psi_\beta(\mathbf{y}, t) \right] = \left[\psi_\alpha^\dagger(\mathbf{x}, t), \psi_\beta^\dagger(\mathbf{y}, t) \right] = 0, \tag{23a}$$

and its matrix form,

$$\left[\psi_\alpha(\mathbf{x}, t), \psi_\beta^\dagger(\mathbf{y}, t) \right] = \delta_{\alpha\beta} \delta^3(\mathbf{x} - \mathbf{y}), \tag{23b}$$

where α and β denote the spinor components of ψ. Equations (23a) refers to unitarity of the model and Equation (23b) is assumed by the electron-positron transition about the manifolds of BOs in 3D space (Figure 1d). The ψ independent of time in 3D space obeys the uncertainty principle with respect to the electron's position, $\mathbf{p}$ and momentum, $\mathbf{q}$, as conjugate operators (Figure 1c). The commutation relationship of $\mathbf{p}$ and $\mathbf{q}$ is,

$$\{ a_{\mathbf{P}}^r, a_{\mathbf{q}}^{s\dagger} \} = \{ b_{\mathbf{p}}^r, b_{\mathbf{q}}^{s\dagger} \} = (2\pi)^3 \delta^{rs} \delta^3(\mathbf{p} - \mathbf{q}). \tag{24}$$

Equation (24) incorporates both matter and antimatter and their translation to linear time (Figure 3b). The electron as a physical entity generates a positive-frequency such as,

$$\begin{aligned} &\langle 0 | \psi(x) \bar{\psi}(y) | 0 \rangle \\ &= \langle 0 | \int \frac{d^3p}{(2\pi)^3} \frac{1}{\sqrt{2E_{\mathrm{p}}}} \sum_r a_{\mathrm{p}}^r u^r(p) e^{-ipx} \\ &\times \int \frac{d^3q}{(2\pi)^3} \frac{1}{\sqrt{2E_{\mathrm{q}}}} \sum_s a_{\mathrm{q}}^{s\dagger} \bar{u}^s(q) e^{iqy} \; | 0 \rangle. \end{aligned} \tag{25}$$

Equation (25) could explain the dominance of matter (electron) over antimatter if the latter is accorded to the conceptualization process of Dirac fermion provided by the model (e.g., Figs. 2a and 2b).

Preprints.org (www.preprints.org) | NOT PEER-REVIEWED | Posted: 18 June 2024 doi:10.20944/preprints202210.0172.v10

Non-relativistic wave function. Observation by light-matter interaction allows for the emergence of the model from the point-boundary at Planck length. Subsequent energy shells of BOs at the n-levels by excitation accommodates complex fermions, ±1/2, ±3/2, ±5/2 and so forth (Figure 4a). The orbitals of 3D are defined by total angular momentum, $\vec{J} = \vec{l} + \vec{s}$ and this incorporates both orbital angular momentum, l and spin angular momentum, s (Figure 4b). These are aligned with Schrödinger wave function (e.g., Figure 1c). The reader is also referred to Appendices, A, B and C. Within a hemisphere, the model is transformed to a classical oscillator. By clockwise precession, a holographic oscillator from the other hemisphere of the MP field remains hidden. One oscillator levitates about the other (Figure 4b) and both are not simultaneously accessible to observation by Fourier

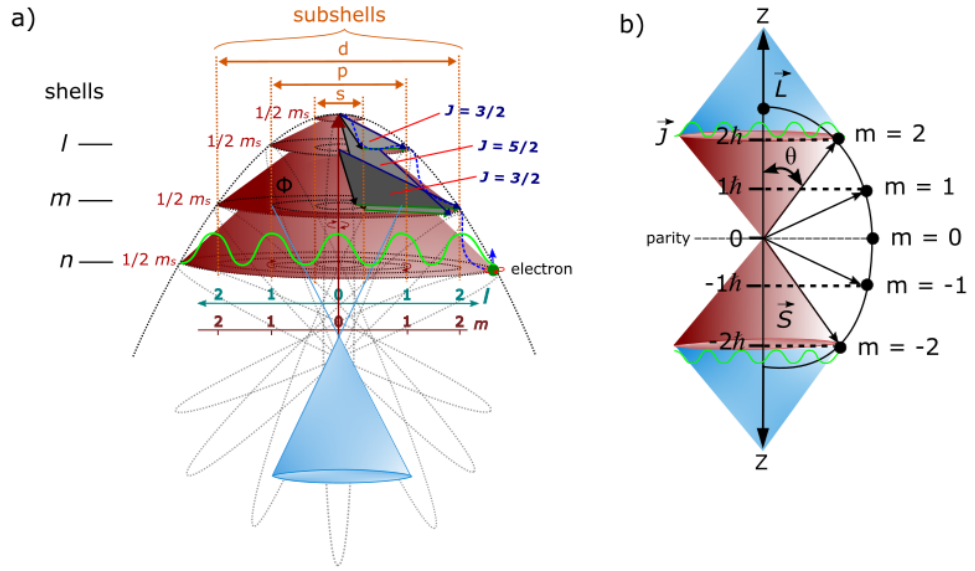

Figure 4. Light-MP model coupling. (a) To an external observer, the topological point-boundary provides the origin for the emergence of the oscillator (maroon light cones). Total angular momentum, $J_z = S + L$ is minimal with S and L in opposite directions. Increase into n-dimensions, k to l offers asymptotic boundary to the energy shells and subshells inclusive of the hidden oscillator. The BOs in degeneracy, Φ_i (see also Figure 1d) at the n-levels can accommodate Fermi-Dirac statistics (green wavy curve) and possibly Fock space for non-relativistic many-particle systems if multielectron are assigned to multiple MP fields. The observable oscillator is partitioned at the infinite boundary at the center of the MP field and is equivalent to classical limit. The blue light cone is from the perspective of the observer at the center and is relevant to Schrödinger wave function (e.g., Figure 1c). (b) The emergence of quantized magnetic moment, $\pm J_z = m_j \hbar$ from the point-boundary (maroon light cones) levitates about the internal frame of the model (blue light cones). Parity transformation for the conjugate pairs is confined to a hemisphere (e.g., Figs. 2a and 2b) and it is related to z-axis of nuclear isospin. Minimal scatterings (green wavy curves) are applicable to light-MP model interactions along the BOs for the eigenfunction, $\vec{J} = \vec{L} + \vec{S}$. transform (e.g., Figure 3b). The n-levels for the fermions can be pursued for Fermi-Dirac statistics with the point-boundary assigned to zero-point energy (ZPE). The $\pm\vec{J}$ splitting (Figure 4a) can apply to Landé interval rule due to the electron isospin and this can somehow accommodate lamb shift and thus, hyperfine structure constant. Such a scenario is similar to how vibrational spectra of a harmonic oscillator for diatoms like hydrogen molecule incorporates rotational energy levels. The difference of the classical oscillator to the quantum scale is the application of Schrödinger wave equation (e.g., Figure 1c).

Weyl spinor. The light cone from the point-boundary within a hemisphere accommodates both matter and antimatter by parity transformation to generate Dirac spinor (Figs. 1c, 2a–d and 4b). It is described in the form,

 doi:10.20944/preprints202210.0172.v10

$$\psi = \begin{pmatrix} \psi_0 \\ \psi_1 \\ \psi_2 \\ \psi_3 \end{pmatrix}. \tag{26}$$

Equation (26) corresponds to spin up fermion, a spin down fermion, a spin up antifermion and a spin down antifermion (e.g., Figs. 2c and 2d). By forming its own antimatter, Dirac fermion somewhat resembles Majorana fermions. It is difficult to observe them simultaneously due to wave function collapse long z-axis of linear time (e.g., Figure 3b). Non-relativistic Weyl spinor of a pair of light cones in 4D space-time are relevant to Schrödinger wave equation in 3D space (Figs. 1c, 3a and 4a). These are defined by reduction of Equation (26) to a bispinor in the form,

$$\psi = \begin{pmatrix} u_+ \\ u_- \end{pmatrix}, \tag{27}$$

where $u_\pm$ are Weyl spinors of chirality with respect to the electron position. By parity operation, $x \rightarrow x' = (t, -\mathbf{x})$, qubits 1 and −1 are generated at the vertices of the MP field (e.g., Figure 1c). Depending on the reference point-boundary of the BO (Figure 1d), the exchanges of left- and right-handed Weyl spinor assumed the process,

$$\begin{pmatrix} \psi'_L \\ \psi'_R \end{pmatrix} = \begin{pmatrix} \psi_R(x) \\ \psi_L(x) \end{pmatrix} \Rightarrow \begin{matrix} \psi'(x') = \gamma^0 \psi(x) \\ \bar{\psi}'(x') = \bar{\psi}(x)\gamma^0. \end{matrix} \tag{28}$$

Conversion of Weyl spinors to Dirac bispinor, ξ^1 ξ^2 are of transposition state (e.g., Figs. 2c and 2d)). The two-component spinor, ξ^1 ξ^2 = 1 are normalized at the point-boundary at position 0 of the spherical model (Figure 1a).

Lorentz transformation. The Hermitian pair, $\psi^\dagger \psi$ of Dirac fermion based on Equation (27) undergo Lorentz transformation in the form,

$$\begin{aligned} u^\dagger u &= (\xi^\dagger \sqrt{p.\sigma},\ \xi \sqrt{p.\bar{\sigma}}\,. \begin{pmatrix} \sqrt{p.\sigma}\xi \\ \sqrt{p.\bar{\sigma}}\xi \end{pmatrix}, \\ &= 2\mathrm{E_P}\xi^\dagger \xi\,. \end{aligned} \tag{29}$$

Equation (29) basically relates to the transformation of the model of 4D space-time to linear time at observation comparable to Fourier transform (e.g., Figure 3b). The corresponding Lorentz scalar applicable to scattering at the BOs (Figure 1d) is,

$$\bar{u}(p) = u^\dagger(p)\gamma^0 \tag{30}$$

Equation (30) is referenced to z-axis as the principle axis of the MP field of a dipole moment in asymmetry (Figure 1c). By identical calculation to Equation (29), the Weyl spinor becomes,

$$\bar{u}u = 2m\xi^\dagger \xi, \tag{31}$$

with respect to the light-cone (Figure 4a). It is difficult to distinguish Weyl spinor and Majorana fermion from Dirac spinor by observations due to superposition of electron-positron pairings (e.g., Figure 2e).

Electroweak symmetry breaking. Coupling of the MP models and ejection of the electron of weak isospin influences COM at position 0 (Figs. 5a and 5b) (see also subsection 2d). The emergence of particle-hole symmetry mimicking the electron may exhibit variation in attraction with the proton. Any adjustments by the proton to accommodate changes in charge and mass is applicable to electroweak symmetry breaking like beta decay of the type, $n^0 \rightarrow p^+ + W^- \rightarrow uud + e^- + \bar{\nu}$ (Figure 6). If charge (e^-) and time by precession are preserved, parity transformation (Figure 4b) would depend on the alignment of the MP field in response to the direction of the applied

Preprints.org (www.preprints.org) | NOT PEER-REVIEWED | Posted: 18 June 2024 doi:10.20944/preprints202210.0172.v10

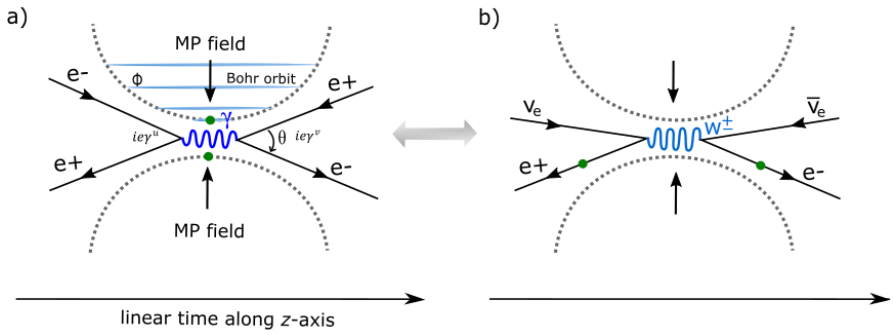

Figure 5. Feynman diagrams of MP models coupling. (a) Two electrons (green dots) or their particle-hole symmetries at the vertices of the MP models may undergo either repulsion or attraction when approaching each other. (b) Ejection of the electron/positron would induce weak particle-hole isospin. COM assumed at the vertices are related to ZPE of classical oscillator (e.g., Figure 4a) and these can generate both bosons and others like neutrinos and antineutrinos of helical property mimicking the electron-positron pair (e.g., Figure 2c and 2d). external magnetic field. The neutrino types (e.g., $\bar{\nu}$) of helical property (Figs. 2c and 2d) would accommodate trivial shift in z-axis, $\langle z|z'\rangle = \delta(z - z')$ (Figure 1d) at precession.

These particles acquire energy, γ or $\frac{-ig_{uv}}{p^2}$ from on-shell momentum ($p^2 = m^2$) tangential to the BO (Figs. 1d and 4a) and this in turn sustains Einstein mass-energy equivalence of the form,

$$E^2 - |\vec{p}|^2c^2 = m^2c^2. \quad (32)$$

Translation to linear time by wave function collapse is normalized to the z-axis (Figure 3b) for particles possessing angular momenta, iey^u, iey^v such as vector bosons, $W^{\pm}$ at short range within the vicinity of the model (Figure 6) during the coupling process (Figs. 5a and 5b). Spin 1 and spin 0 particles are assigned to the point-boundary of ZPE of a classical

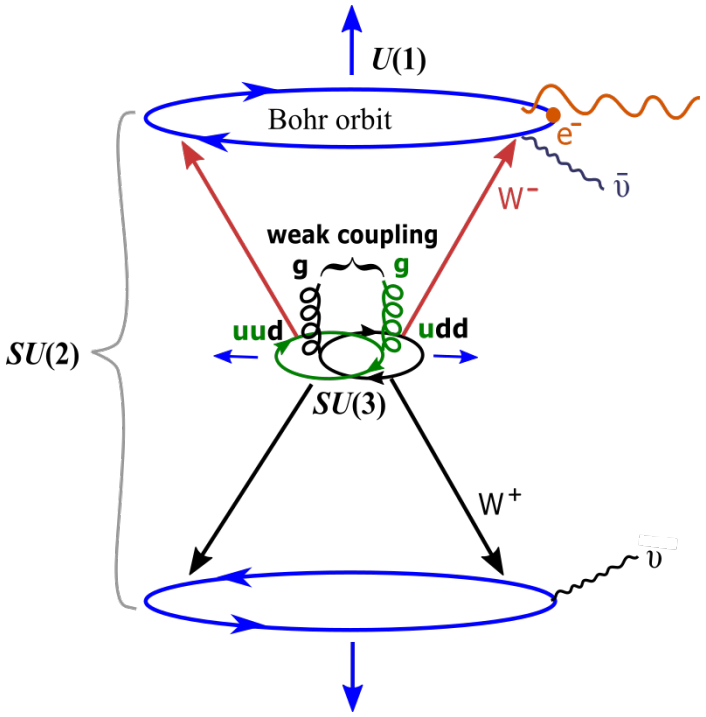

Figure 6. A hypothetical scenario of beta decay from an energized MP model during interaction. The proton and neutron are assumed to mimic the MP field. The charge and color flavor of quarks from exchanges by gluons are short range from on-shell momentum ($p^2 = m^2$) tangential to the BO. The symbols, u = up quark, d = quark and g = gluon. Note, $W^{\pm}$ bosons can align with z-axis of the MP model as nuclear isospin (blue arrows) during precession. oscillator (Figure 4a) and the electron of

 doi:10.20944/preprints202210.0172.v10

spin 1/2 and its translation to leptons is assumed into n-dimensions (Figure 1d). Constriction of the models at high energy towards position 0 (Figs. 5a and 5b) can become massive and this would mimic both $H°$ (see subsection 2d) and Nambu-Goldstone boson by continual precession for changes in mass attained by the particle-hole/electron shift away from z-axis at position 0 via Dirac process (Figure 1d). Quark flavor and color for both proton and neutron could mimic the electron in orbit of the MP model and gluons color-charge tangential to on-shell momentum into n-dimensions (Figure 6). The entangled mini MP models by Dirac process would be reduced to ±1/3 spin of helical property compared to the electron, ± 1/2 spin (e.g., Figs. 2c and 2d). For the irreducible spinor field represented by the MP model, gravity can be considered a classical force. These explanations may form the basis for electroweak symmetry breaking with variations in mass and charge for a plethora of particles from on-shell momenta as a consequence of applied external energy, magnetic field and the type of matter under observation. The particles' relationships to vectors, matrices and tensors associated with QFT are demonstrated in Figure 2A (Appendix B). Such a notion looks promising to link nuclear physics, high and low energies physics for electroweak breaking of SU(3) x SU(2) x U(1) symmetry (Figure 6). Similarly, any deviations in the magnetic moment of the electron by continual precession can account for the fine-structure constant, $a = \frac{e^2}{\hbar c} = \frac{e^2}{4\pi} \approx \frac{1}{137}$ such as the lamb shift and this is relevant to pursuits in quantum electrodynamics.

4. Conclusions

The dynamics of the MP model of 4D space-time offered in this study allows for the transformation of the electron of hydrogen atom type to Dirac fermion of a complex four-component spinor. It consists of clockwise precession of an elliptical MP field of Dirac string with the electron in orbit and this generates a spherical model of space-time. The orbit of time reversal against precession insinuates both the Dirac belt trick and its solenoidal property into n-dimensions is relevant to the emergence of monopoles in situ of the model. Such a tool is shown to be compatible with basic interpretations of quantum mechanics, Lie group and field theory and their related components like wave function collapse, quantized Hamiltonian, non-relativistic wave function, Weyl spinor, Lorentz transformation and electroweak symmetry breaking mechanism. Though the model remains a speculative tool, it can become important towards defining the fundamental state of matter and its field theory subject to further investigations by conventional methods in both experiment and theoretical applications.

Data availability statement: The modeling data attempted for the current study are available from the corresponding author upon reasonable request.

Competing financial interests: The author declares no competing financial interests.

Appendix A. Mathematical property of Schrödinger wave equation

The Schrödinger equation cannot be derived similar to Newton's law of gravity. Its mathematical property can be plotted [23] beginning with the normalized sine wave function,

$$\psi = Asin\frac{2\pi x}{\lambda}, \tag{A1}$$

where A is the amplitude shown in Figure 1A. Its second derivation is,

$$\frac{d^2\psi(x)}{dx^2} == \frac{-4\pi^2}{\lambda^2}\psi(x). \tag{A2}$$

Velocity, v can be calculated from total energy in the form,

$$v^2 = \frac{2(E-V)}{m}, \tag{A3}$$

 doi:10.20944/preprints202210.0172.v10

where V is potential energy and kinetic energy is, $\frac{1}{2}mv^2$. Taking the squared function of de Broglie relationship becomes,

$$\lambda^2 = \frac{h^2}{m^2v^2}. \quad \text{(A4i)}$$

By substitution from Equation (3A), Equation (4A(i)) can be rewritten as,

$$\lambda^2 = \frac{h^2}{2m(E-V)}. \quad \text{(A4ii)}$$

By substitution into Equation (2A), this becomes,

$$\frac{d^2\psi(x)}{dx^2} == \frac{-8m\pi^2}{h^2}(E-V)\psi(x). \quad \text{(A5i)}$$

An alternative form of Equation (5A(i)) is,

$$-\frac{\hbar}{2m}\frac{\partial^2}{\partial x^2} + V\psi(x) = \frac{p^2}{2m}\psi(x) = E\psi(x). \quad \text{(A5ii)}$$

By first derivation of space-time due to clockwise precession of the MP model (Figure 1c), Equation (5A(ii)) is given by,

$$i\hbar\frac{\partial}{\partial t}(\psi(\vec{r})\theta(t) = E\psi. \quad \text{(A5iii)}$$

In this way, the model offers physical meaning to Schrödinger wave equation as an eigenvalue of ψ similar to Newton's law of gravity with the electron of isospin represented by, i or $2m$.

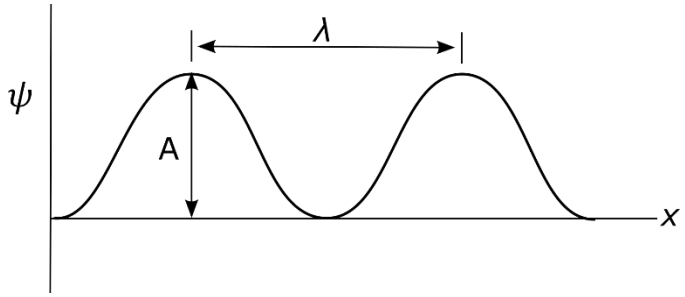

Figure A1. Translation of a sine wave function along x-axis.

Appendix B. Basis of vectors, matrices, tensors and Fourier transform

The physicality of the complexity of Dirac four-component spinor can somehow relate to the MP model. The BOs provide the basis for vector to multivector into n-dimensions or n-energy levels along z-axis (Figure 2A). By rotation, the BOs generate both spin up and spin down and these are

Preprints.org (www.preprints.org) | NOT PEER-REVIEWED | Posted: 18 June 2024 doi:10.20944/preprints202210.0172.v10

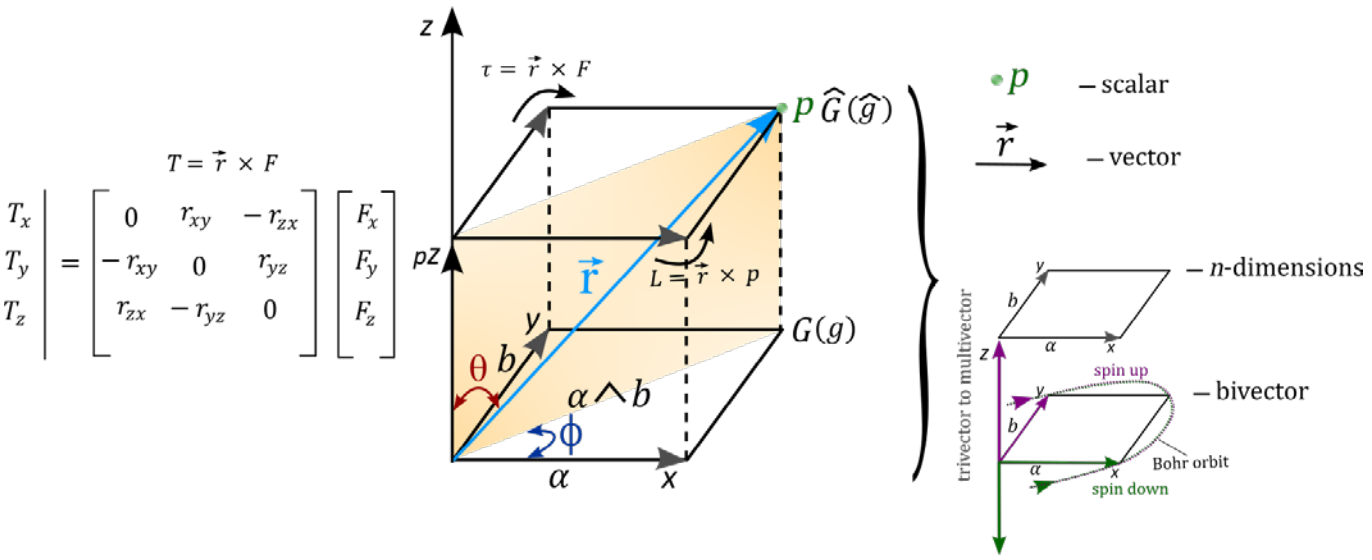

Figure 2. A. The basis of vectors to multivectors, matrices, tensors and Fourier transform. The vectors are aligned with either spin up or spin down by rotation of the BO. Translation along z-axis of nuclear isospin provides trivectors to multivector into n-dimensions of unidirectional. The matrices are related to tensors along z-axis by Fourier transform for the commutation, pZ to Z (see text for details). The $\vec{r}$ is a four 3-fold rotational axis (shaded orange plane) in 3D of the box and is applicable to Fourier transform (e.g., Figure 3b). It mimics a 4-gradient Dirac operator, ∇ for vectors to multivector into n-dimensions of the box (see also red rectangle in Figure 1c). Rotation into forward time, $\tau = \vec{r} \times F$ is by clockwise precession and this insinuates spin up with the unfolding process for spin down by, $L = \vec{r} \times p$. The spin rotation matrices applicable to Clifford algebra are shown to the left. The half-integer spins of SU(2) group provide double cover (bivector) with shift in both θ and ϕ into n-dimensions for the Lie group ladder operators, $G(g)$ and $\hat{G}(\hat{g})$. Some key features of the dimensional box are expounded to the right.

Assumed into n-dimensions of a box (Figure 2A). The rotation by $\vec{r}$ is a four 3-fold axis in 3D and its matrices are defined by Cartesian coordinates, x, y and z. These are related to shift in both θ and Φ as double cover of SU(2) for vector to multivectors assumed within the BOs. They are applicable to the Lie group ladder operators, $G(g)$ and $\hat{G}(\hat{g})$ of 3D space and 4D space-time. By linearization akin to Fourier transform (e.g., Figure 3b), the boxes of isomorphism consisting of BOs are translated along the z-axis (Figure 2A). The BO of bivector field is related to z/pz of integers modulo p of prime. The shift along z-axis of isospin is commutative (Figure 2A) and any changes by precession is trivial and is reduced to the MP field of Dirac string (e.g., Figure 1d). The MP field of irreducible representation, Π is given by [21],

$$\rho(g) = [\Pi(\hat{g})], \tag{A6}$$

where ρ is composed of algebraic structure (pz, $+p$ and xp) for vectorization, V into p-dimensional space defined by $\alpha \wedge b$ (Figure 2A). The two operators, T_a and S_a acting on V are

$$(T_a f)(b) = f(b - a) \tag{A7i}$$

and

$$(S_a f)(b) = e^{2\pi i a b} f(b), \tag{A7ii}$$

where T is identified by the rotational matrices, $T = \vec{r} \times F$ (Figure 2A) and S_a is the shift in frequency in space along z-axis (e.g., Figure 3b). These intuitive demonstrations somehow provide a geometry perspective to the MP model with its relevance to the Lie group mentioned in the article (see subsection 2c).

Appendix C. Vector modelling of the MP model

Preprints.org (www.preprints.org) | NOT PEER-REVIEWED | Posted: 18 June 2024 doi:10.20944/preprints202210.0172.v10

Schrödinger wave equation forms the basis of quantum mechanics and offers satisfactory explanations to account for probability distribution or orbitals of subatomic particles like electrons in the atom. However, quantum mechanics cannot account for the combination of orbital angular momenta, spin angular momenta and magnetic moments of valence electrons observed in atomic spectra. Russell-Saunders orbital-spin (L-S) coupling ensues by Clebsch-Gordon series such as for the eigenvalue of total angular momentum, $\vec{J} = \vec{l} + \vec{s}$, and this incorporates eigenvalues of both orbital angular momentum, l and spin angular momentum, s.

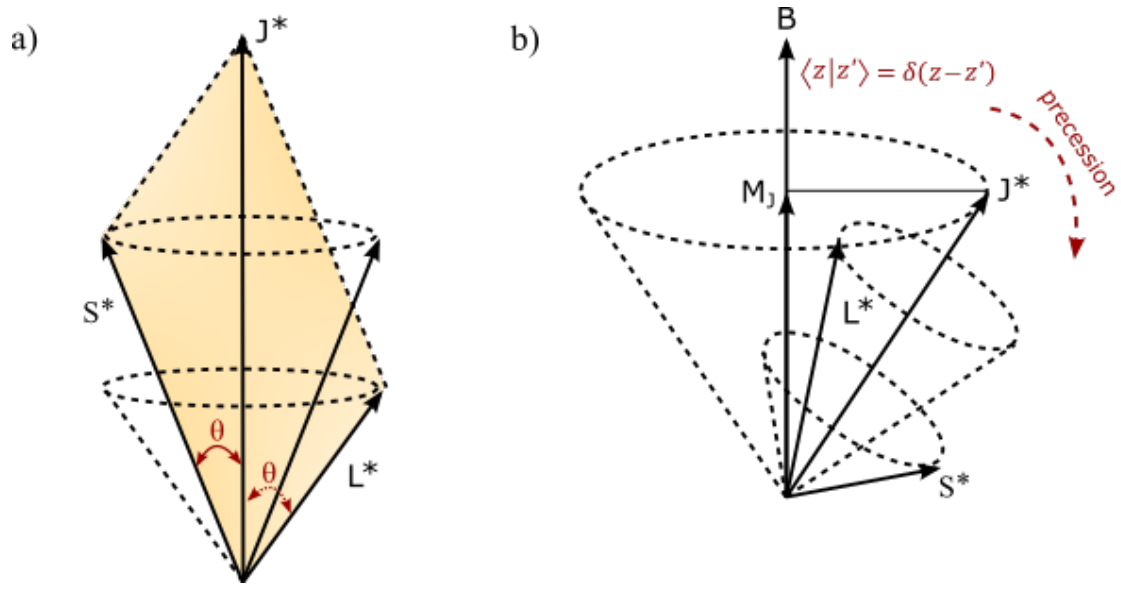

Figure 3. A. Vectors of orbital angular momentum. (a) Vectors **L** and **S** precess about this resultant **J**. In other words, any precession affecting **L** and **S** in the form, $\langle z|z'\rangle = \delta(z - z')$ is reduced to the MP field of magnetic property such as Dirac string along z-axis. The shaded area of bivector from Figure 2A is extended to the point-boundary of the MP model (see also Figure 4a). (b) Vector J of the MP field precesses in correspondence to applied external magnetic field **B**. Both images are adapted from ref. [24].

From the emergence of the oscillator at the point-boundary (Figure 4a), the n-dimensions can cater for both the resultant orbital angular momentum, **L** and resultant spin angular momentum, **S**, where spin-orbit interaction is related to constant shift in the electron position and its link to BO into n-dimensions (Figure 4a). Complete rotation towards the point-boundary by Dirac process is twice, 2π and the positron-electron transition is related to h. The lone valence electron of the MP model akin to hydrogen atom by precession takes the form,

$$|l| = \sqrt{l_i(l_i + 1)}\hbar, \qquad \text{(A8i)}$$

where i is equal to the subshells (Figure 4a). For example, $n = 2$ is split into s and p orbitals with each one accommodating spin 1/2 and from electron-positron transition of Dirac process at spherical lightspeed (Figure 1a), this equates to ±1/2 spin in accordance with Pauli exclusion principle. The total angular momentum, $\vec{J} = l \pm \frac{1}{2}$, is $\frac{3}{2}$ and $\frac{1}{2}$ at $n = 2$, $l = 1$. The former is assumed from the summation of spin, 1/2 + 1/2 + 1/2 from combined s and p subshells by $n_2 + n_1 = \frac{3}{2}$, when both orbital and spin angular momenta are aligned in the same direction (Figure 4b). It also provides the magnitude of **S**. The latter of low energy from $n_2 - n_1 = \frac{1}{2}$ in the form, 1/2 + 1/2 − 1/2 and is assigned to p orbital by cancelling out 1s orbital. This does not consider the orientation such as of the p subshells into n-

 doi:10.20944/preprints202210.0172.v10

dimensions (e.g., Figure 4a). The corresponding **L** from the combination of $\sum l_i$ in a complete loop of BO at *n*-dimension is,

$$|\mathbf{L}| = \sqrt{\mathbf{L}_n(\mathbf{L}_n + 1)}\hbar, \tag{A8ii}$$

where the values of 0, $\sqrt{2}\hbar$ and $\sqrt{6}\hbar$ are generated at $n = 0$ to $n = 2$. Their projection with respect to *z*-axis for the irreducible MP field is,

$$|\mathbf{L_Z}| = M_L\hbar. \tag{A8iii}$$

Equation (8A(iii)) is applicable to the light cone and the same is projected for $\vec{J}$ such as,

$$J_Z = m_l\hbar, \tag{A9i}$$

where m_l can take $(2l + 1)$ values in both equations as eigenfunciton of M_L. Both **S** and **L** combine to generate **J** in the form,

$$\mathbf{J} = \mathbf{L} + \mathbf{S}. \tag{A9ii}$$

Distinction of **L** and **S** are provided in Figure 4b and the orientations by precession are applicable to M_L. These explanations can possibly account for odd fermion spin types such as, $\frac{1}{2}, \frac{3}{2}, \frac{5}{2}$ noted for Zeeman effect (e.g., Figure 4a) and also lamb shift from the electron-positron transition in discreet form (e.g., Figure 3c). In this case, the electron is of weak isospin and *z*-axis is applicable to nuclear isospin. Both are linked to BOs into *n*-dimensions and these are subjected to the twisting and unfolding process by Dirac process (Figs. 1a and 1b).

References

1. Peskin, M. E. & Schroeder, D. V. *An introduction to quantum field theory*. Addison-Wesley, Massachusetts, USA (1995). pp 13–25, 40–62.
2. Alvarez-Gaumé, L. & Vazquez-Mozo, M. A. Introductory lectures on quantum field theory. *arXiv preprint hep-th/0510040* (2005).
3. Pawłowski, M. et al. Information causality as a physical principle. *Nature* **461**(7267), 1101-1104 (2009).
4. Henson, J. Comparing causality principles. *Stud. Hist. Philos M. P*, **36**(3), 519-543 (2005).
5. Nelson, E. Derivation of the Schrödinger equation from Newtonian mechanics. *Phys. Rev.* **150**(4), 1079 (1966).
6. Li, Z. Y. Elementary analysis of interferometers for wave—particle duality test and the prospect of going beyond the complementarity principle. *Chin. Phys. B* **23**(11), 110309 (2014).
7. Rabinowitz, M. Examination of wave-particle duality via two-slit interference. *Mod. Phys. Lett. B* **9**(13), 763-789 (1995).
8. Rovelli, C. Space is blue and birds fly through it. *Philos. Trans. Royal Soc. Proc. Math. Phys. Eng.* **376**(2123), 20170312 (2018).
9. Perkins, D. H. Proton decay experiments. *Ann. Rev. Nucl. Part. Sci.* **34**(1), 1-50 (1984).
10. Sun, H. Solutions of nonrelativistic Schrödinger equation from relativistic Klein–Gordon equation. *Phys. Lett. A* **374**(2), 116-122 (2009).
11. Oshima, S., Kanemaki, S. & Fujita, T. Problems of Real Scalar Klein-Gordon Field. *arXiv preprint hep-th/0512156* (2005).
12. Bass, S. D., De Roeck, A. & Kado, M. The Higgs boson implications and prospects for future discoveries. *Nat. Rev. Phys.* **3**(9), 608-624 (2021).
13. Weiss, L. S. et al. Controlled creation of a singular spinor vortex by circumventing the Dirac belt trick. *Nat. Commun.* **10**(1), 1-8 (2019).
14. Silagadze, Z. K. Mirror objects in the solar system?. *arXiv preprint astro-ph/0110161* (2001).
15. Rieflin, E. Some mechanisms related to Dirac's strings. *Am. J. Phys.* **47**(4), 379-380 (1979).
16. Yuguru, S. P. Unconventional reconciliation path for quantum mechanics and general relativity. *IET Quant. Comm.* **3**(2), 99–111 (2022).
17. Jaffe. R. L. Supplementary notes on Dirac notation, quantum states, etc. https://web.mit.edu/8.05/handouts/jaffe1.pdf (September, 2007).
18. Eigen, C. Spinors for beginners. https://www.youtube.com/@eigenchris (November, 2012)
19. Zhelobenko, D. P. Compact Lie groups and their representations. *J. Amer. Math. Soc.* **40**, 26-49 (1973).
20. https://en.wikipedia.org/wiki/Spinor (updated February 2024).

 doi:10.20944/preprints202210.0172.v10

21. Burdman, G. Quantum field theory I_Lectures. http://fma.if.usp.br/~burdman (October, 2023).
22. Das, I. et al. *An introduction to physical chemistry*. New Age International (P) Limited, New Delhi, India (2005) 2nd Ed. pp 16-20.
23. Singh, R. B. *Introduction to modern physics*. New Age International (P) Limited, New Delhi, India (2009) 2nd Ed. Vol. 1, pp 420-425.